

PHYS4070 Project 3: Dynamics of Interacting Quantum Systems

Semester 1 2023, 26 May

Hugh McDougall, 4302007

Contents

Part 1 - Bright Solitons in the Non-Linear Schrödinger Equation.....	2
1.1 – Numerical Modelling of the Non-Linear Schrödinger Equation.....	3
1.2 – Effect of Repulsive Interaction on ‘Particle in a Box’ eigenstates.....	4
1.3 – Stable Solutions & Wave Packets	5
1.4 –Multi-Particle Behaviour	7
Part 2 - The Transverse Ising Spin Model.....	10
2.1 – Numerical Modelling of the Transverse Ising Spin Model.....	13
2.2 – Effect of Interaction & System Size on Ground Energy Function.....	15
2.3 – Time Evolution of Quenched States	16
References	19
Appendix A – Peak-Peak Separations for All Phase Shifts	19

The code for generating the results and plots in this report are contained in separate folders marked for each part, with each folder containing a shell script `_compile_and_run.sh` that should compile the scripts and generate results with the correct naming conventions. Results are saved to the enclosed `./results` folders, which contain python files for generating the relevant plots. For the wave-evolution plots in part 1, animations are generated by the `_plot.py` file, with the user being prompted as to which set of results they want to generate the plots for. Further information on compiling and running the scripts is available in the `readme.pdf` in the docs folder.

Part 1 - Bright Solitons in the Non-Linear Schrödinger Equation

The mechanics of the linear Schrödinger equation are generally considered a solved problem, particularly in the simplest case of a time-static one-dimensional potential. For such a case, the Schrödinger equation becomes a simple linear wave-equation, with the complex components allowing for second order behaviour despite the equation being first order in time:

$$i \frac{\partial \psi(x, t)}{\partial t} = \hat{H} \psi = -\frac{\partial^2 \psi(x, t)}{\partial x^2} + V(x) \psi(x, t)$$

This yields energy eigenstates which time-evolve independently of one another, allowing us to decompose any arbitrary wave into these eigenstates.

$$|\psi(t)\rangle = \sum_i \langle h_i | |\psi(t=0)\rangle e^{-iE_i t} |h_i\rangle, \quad E_i |h_i\rangle = H |h_i\rangle$$

However, this simple behaviour devolves within even simple non-linearity and wave self-interaction. In this report, we examine a simple case of non-linearity in which the wave function imposes its own self-interacting potential term based on its position density:

$$V_{int} = g|\psi|^2$$

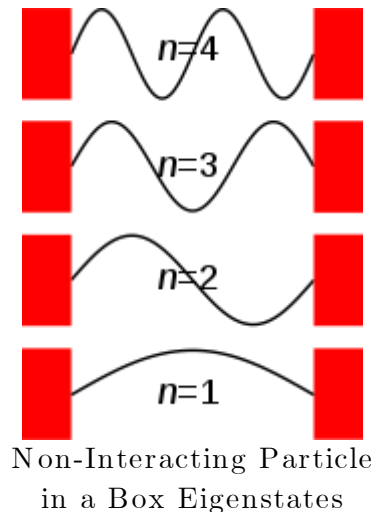
Here, $g > 0$ creates self-repulsive potential ‘bumps’ where the wave particle is most present, motivating it to spread out, and $g < 0$ creates a self-attraction effect. We specifically consider this case as applied to the well-studied ‘particle in a box’ system, a free particle constrained to a finite domain by ‘walls’ of external potential:

$$V_{Ext}(x) = \begin{cases} 0 & |x| < L \\ \infty & |x| > L \end{cases}$$

This forces the system to obey fixed boundary conditions $\psi(x \leq -\frac{L}{2}) = \psi(x \geq \frac{L}{2}) = 0$. For the non-interacting case, this system has well established eigenstates in the form of harmonic waves (e.g. figure right) which evolve independently via the linear time evolution operator:

$$C^n(t) = e^{-iE_i t} C^n(t=0),$$

$$C^n = \begin{cases} \cos\left(n \frac{\pi}{L} x\right) & n \text{ is odd} \\ \sin\left(n \frac{\pi}{L} x\right) & n \text{ is even} \end{cases}$$



In this report, we model the impact of the self-interaction term on the eigenstates of the particle in a box, and examine the eigenstates of coherent wave-packets and time evolution of multi-wave systems.

1.1 – Numerical Modelling of the Non-Linear Schrödinger Equation

To model the dynamics of the Schrödinger equation, we divide the wave state into a 1D grid of N discrete points in the domain $x \in \left[-\frac{L}{2}, \frac{L}{2}\right]$, enforcing the boundary conditions of the particle in a box potential:

$$\psi_0(t) = \psi\left(x = -\frac{L}{2}\right) = 0, \quad \psi_{N-1}(t) = \psi\left(x = \frac{L}{2}\right) = 0$$

In this example we use $L = 20$. We can evolve the wave-state using the Schrödinger equation to evaluate time-derivatives:

$$\frac{\partial \psi_i(t)}{\partial t} = -i\hat{H}\psi_i(t) = i\frac{\partial^2 \psi_i(t)}{\partial x^2} + ig|\psi_i(t)|^2 \psi_i(t)$$

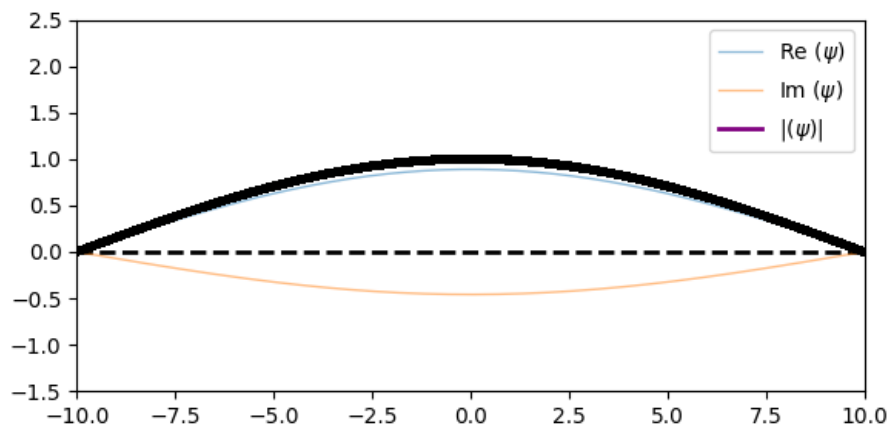
Where we approximate the wave curvature with a finite difference equation:

$$\frac{\partial^2 \psi_i(t)}{\partial x^2} \approx \frac{\psi_{i+1}(t) - 2\psi_i(t) + \psi_{i-1}(t)}{N+1}$$

Note that the boundary conditions imply $\left[\frac{\partial \psi_i(t)}{\partial t}\right]_{0,N-1} = 0$, which also enforces $\frac{\partial^2 \psi_i(t)}{\partial x^2} = 0$ at these points.

Integration is then performed using the fourth order Runge Kutta method, a fixed step-size integrator which uses a nested series of estimates of $\frac{\partial \psi_i(t)}{\partial t} \psi_i$ to minimize truncation error in each step:

$$\psi_i(t + \Delta t) = \psi_i(t) + \left(\frac{\vec{k}_1}{3} + \frac{\vec{k}_2}{6} + \frac{\vec{k}_3}{6} + \frac{\vec{k}_4}{6}\right) \Delta t \quad \left| \quad \begin{aligned} k_1 &= -i\hat{H}\psi_i(t) \\ k_2 &= -i\hat{H}\psi_i\left(t + \frac{\Delta t}{2}k_1\right) \\ k_3 &= -i\hat{H}\psi_i\left(t + \frac{\Delta t}{2}k_2\right) \\ k_4 &= -i\hat{H}\psi_i(t + \Delta tk_3) \end{aligned} \right.$$

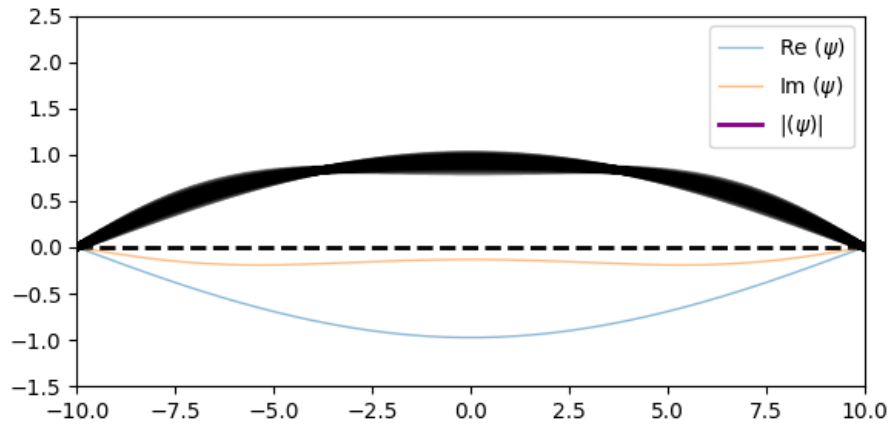


Time-Static Half-Cos Wave State for $g = 0$. This is the lowest energy state of a non-interacting particle in a box.

1.2 – Effect of Repulsive Interaction on ‘Particle in a Box’ eigenstates

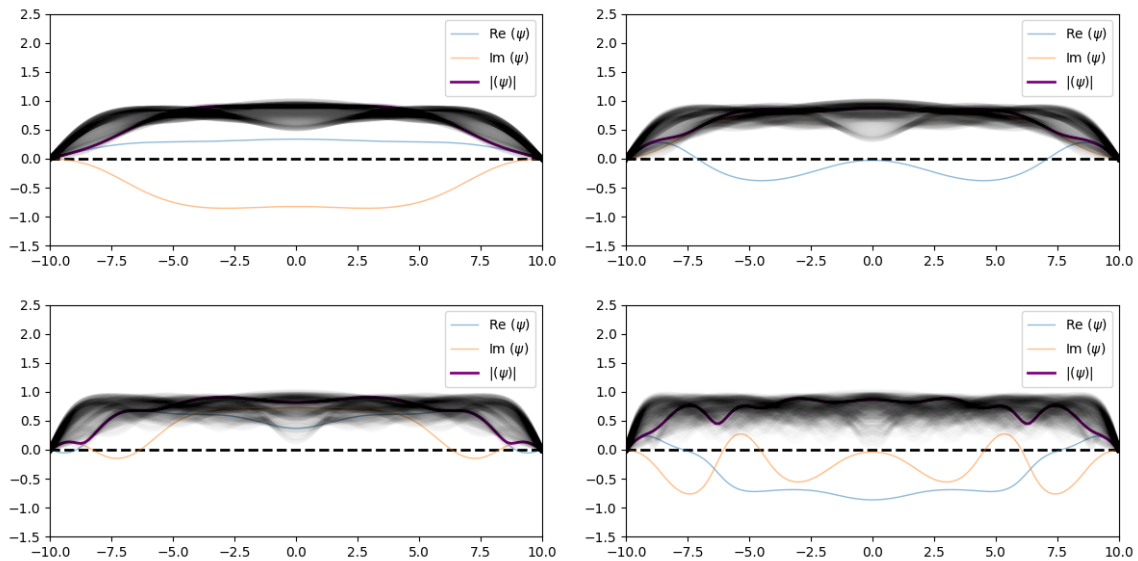
In this section, we test the effects of a repulsive $g > 0$ interaction of increasing strength on the particle in a box wave-states. To first order, we can imagine the self-interaction as being similar to adding static potential ‘bump’, $V_{bump}(x) \propto \cos^2\left(\frac{\pi x}{L}\right)$, which drives the cos-wave away from the centre.

This perturbation causes a ‘mixing’ of the modes, with the $n=1$ half-cos wave to now bleeding into the $n=3$ mode, shown below as a three-node ‘wobble’ on top of the initial wave state. This figure, and others like it, shows an overlay of the wave norm at multiple times as a series of ‘shadows’ to give an impression of the time varying behaviour.



Time evolution of the $g = 0.1$ system prepared in a half-cos wave.

Note that the symmetry of our initial state means that we can only excite odd numbered symmetrical modes. As we increase the interaction strength, this trend continues: higher and higher order modes are excited, all symmetrical, causing the system to gradually decohere into mess of short wavelength, high frequency waves.



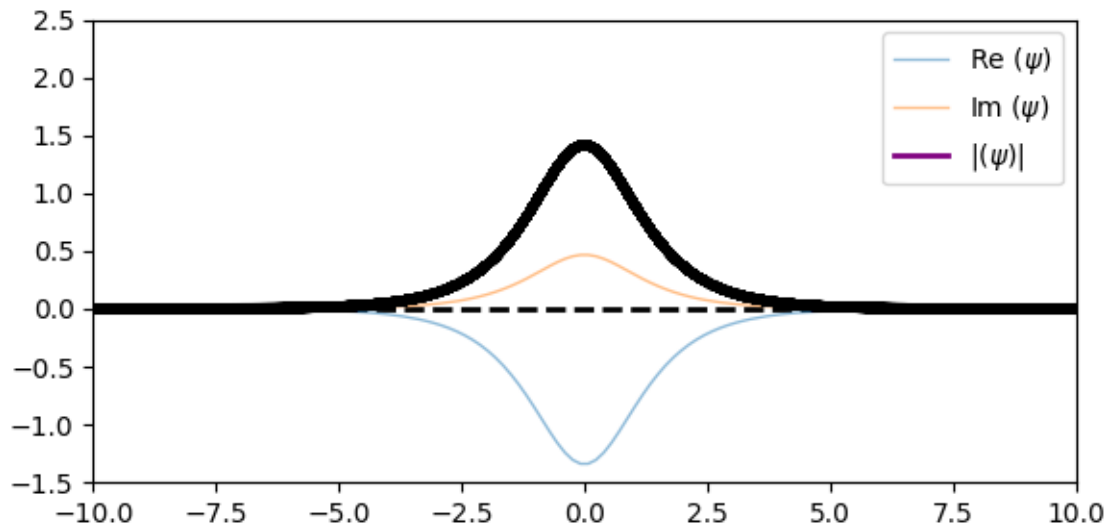
Time Evolution of System Prepared in Half-Cos Wave at, from top left, $g = 0.5$, $g = 1.0$, $g = 2.0$, $g = 5.0$

1.3 – Stable Solutions & Wave Packets

When using an attractive interaction with $g = -1$, a new time-stable eigenstate becomes possible. The self-attractive causes this eigenstate's to draw inwards compared to the non-interacting case, forming a compact wave-packet given by:

$$\psi(t = 0, x) = \sqrt{2} \operatorname{sech}(x) = \sqrt{2} \frac{1}{\cosh(x)}$$

Much like the cos-wave eigenstates of the non-interacting particle, this wave packet is stationary in time, evolving in time only with a phase modulation. Note that this solution goes to zero as $x \rightarrow \infty$, and as such obeys not only the box-like boundary conditions, but is also so is a valid solution for any ‘flat’ potential.



Sech-wave at $u = 0$, evolving only in phase.

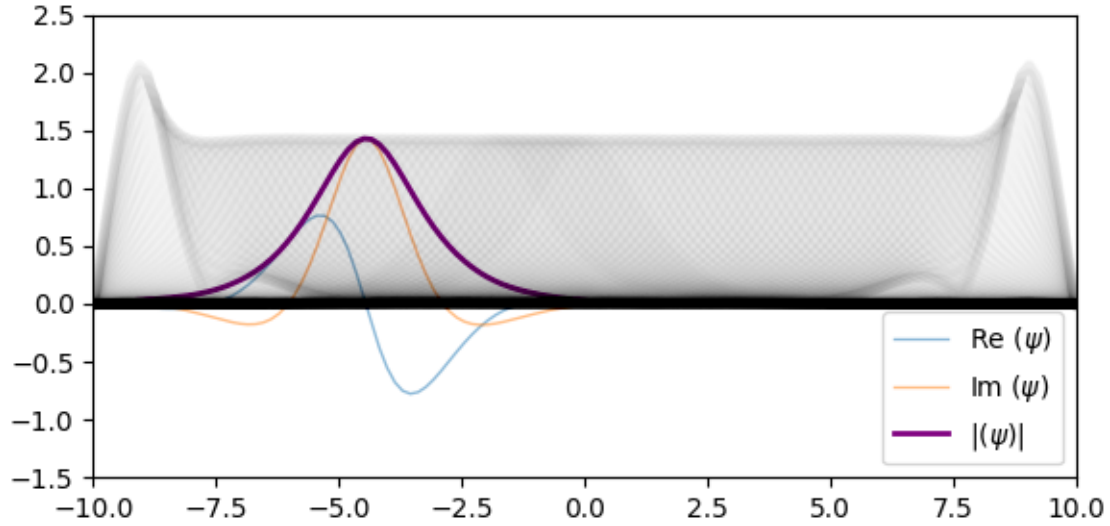
In the same way that energy creates a time-evolution operator that modulates the wave temporally, there is a similar effect when the wave is modulated spatially, i.e.

$$\psi(t = 0, x) \rightarrow e^{iux} \cdot \psi(t = 0)$$

This phasor modulation imparts momentum onto the particle, with positive momentum ($u > 0$) imposing positive (right-bound) momentum. If we apply this to the otherwise stationary sech-wave:

$$\psi(t = 0, x) = \sqrt{2} e^{iux} \operatorname{sech}(x)$$

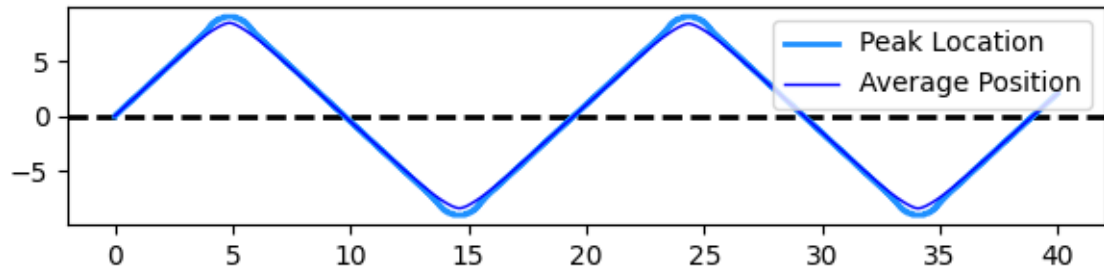
We generate a stable wave packet that propagates through the box, reflecting off the boundary due to the ‘wall’ conditions.



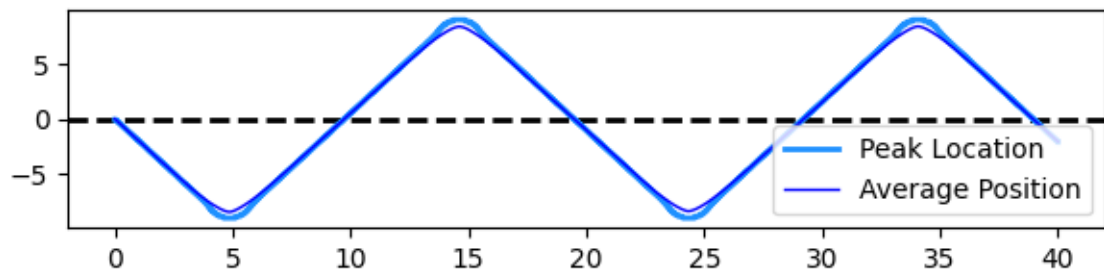
Snapshot / overlay of wave evolution for $u = 1$ sech-wave

Unlike the standing waves of the perturbed half-cos wave initial state, we can clearly see reflection occurring at the system boundaries. The wave packeted spikes in amplitudes as it reflects back on itself, something physically akin to the way a water-wave ‘splashes’ against the edges of its container.

Tracking the location of this wave-packet over time, we can see that $u = 1$ and $u = -1$ give symmetrical results, differing only in the initial direction of the wave-packet motion.



Time



Time

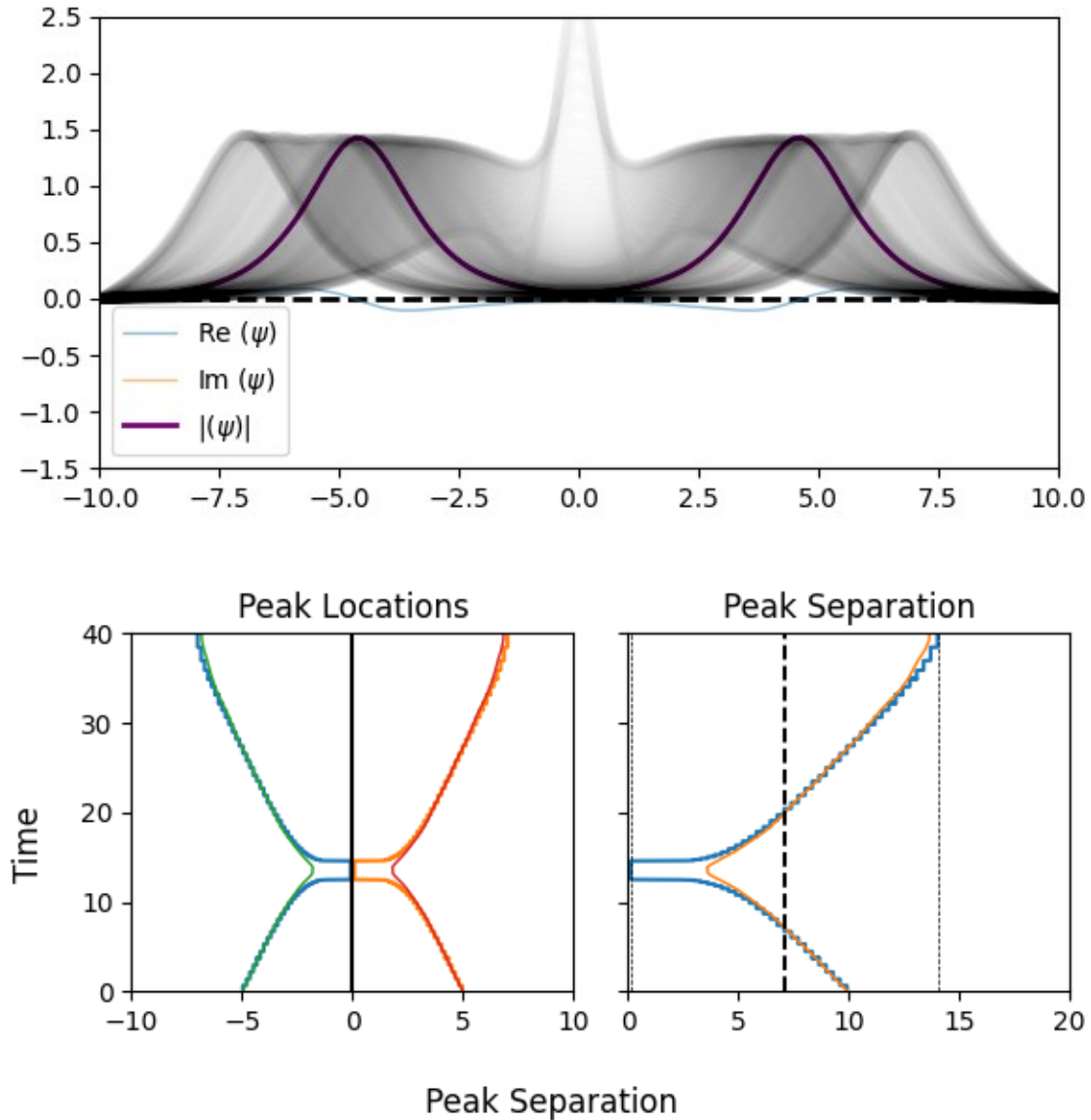
Position of wave packet against time for $u = 1$ (top) and $u = -1$ (bottom)

1.4 –Multi-Particle Behaviour

Previously, we found that stable wave-packets were possible, which we can easily interpret as particle-like objects propagating back and forth in the potential well. This motivates us to consider cases with multiple such particles to see how they interact with one another. In this section, we model two sech-wave packets with opposing momenta, separated by distance $\frac{L}{2}$:

$$\psi(t = 0, x) = \sqrt{2}e^{iux} \operatorname{sech}\left(x + \frac{L}{4}\right) + \sqrt{2}e^{-i[ux-\theta]} \operatorname{sech}\left(x - \frac{L}{4}\right)$$

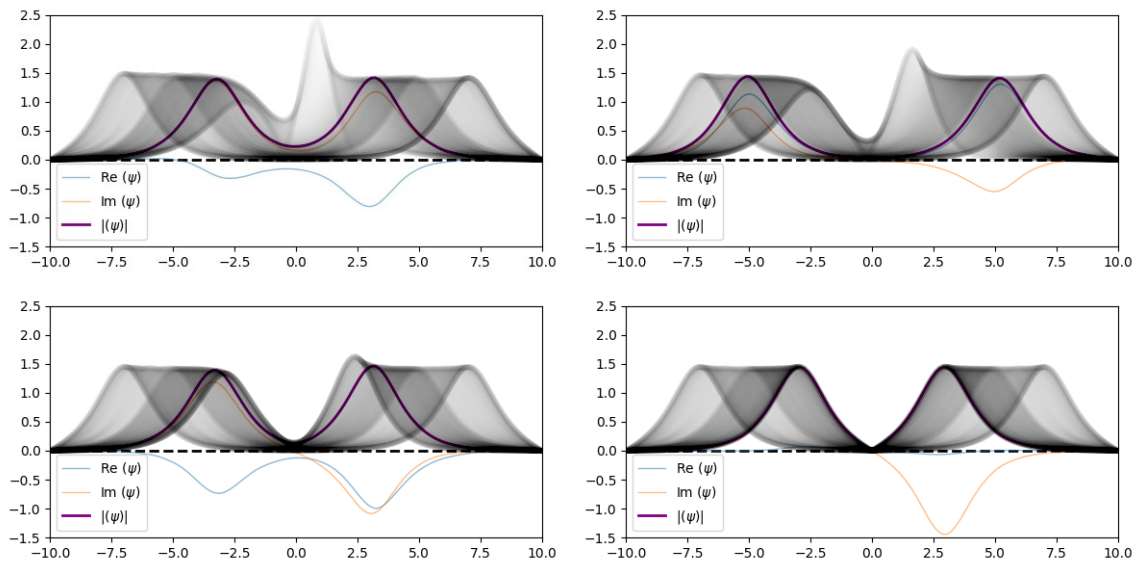
Where we use a lower momentum, $u = 0.1$, to better observe the motion. At $\theta = 0$, we have two identical particles headed directly for one another as an initial condition, and this, expectedly, causes the two wave packets to ‘spike’ as they collide. As the two packets / particles are indistinguishable, this can be equally interpreted either as them passing through one another, or reflecting back on themselves as they do at the system’s walls.



Wave Behaviour (Top) & Peak-Peak Separation (Bottom) for $\theta = 0$ two-particle systems

We can also see the attraction between the wave packets causes them to accelerate towards one another as they close in. In the previous plot, we show the packet location as estimated by the peak (highest point at $x < 0$ or $x > 0$ at any given time-step) and by the average (mean position of wave for $x < 0$ and $x > 0$). The peak position has a rough, stepped, appearance due to the finite spacing of the grid-points. The collapse to ‘zero’ separation in the peak separation at $t \approx 12$ represents a full merge of the two wave packets.

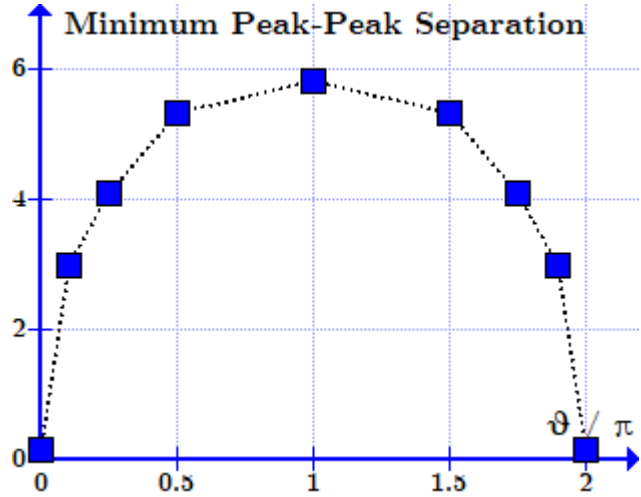
Interesting effects arise when we introduce a phase-shift between the particles. As the particle are moved further out of phase with one another (i.e. as θ increases) a repulsive effect appears that imposes a minimum separation on the wave-packets. As this happens, the ‘bounce’ at closest approach becomes less prominent, until at $\theta = \pi$, i.e. a complete 180° phase difference, the particles have no ‘collision’ at all.



Wave packet evolution for varying phase differences. From top left, $\theta = 0.1\pi$, 0.25π , 0.5π and π .

At a physical level, this apparent repulsion can be interpreted as a being analogous to constructive / destructive interference in a linear system. As the waves approach one another, their real / complex components can ‘cancel out’ near $x \approx 0$. Through a more mathematical lense, we can see that $\theta = 0$ imposes a symmetrical system, while $\theta = \pi$ causes antisymmetry. Antisymmetric systems have the condition $\psi(x = 0) = 0$, enforcing a node in at the centre of the box, and ensuring the wave-packets are fully separate.

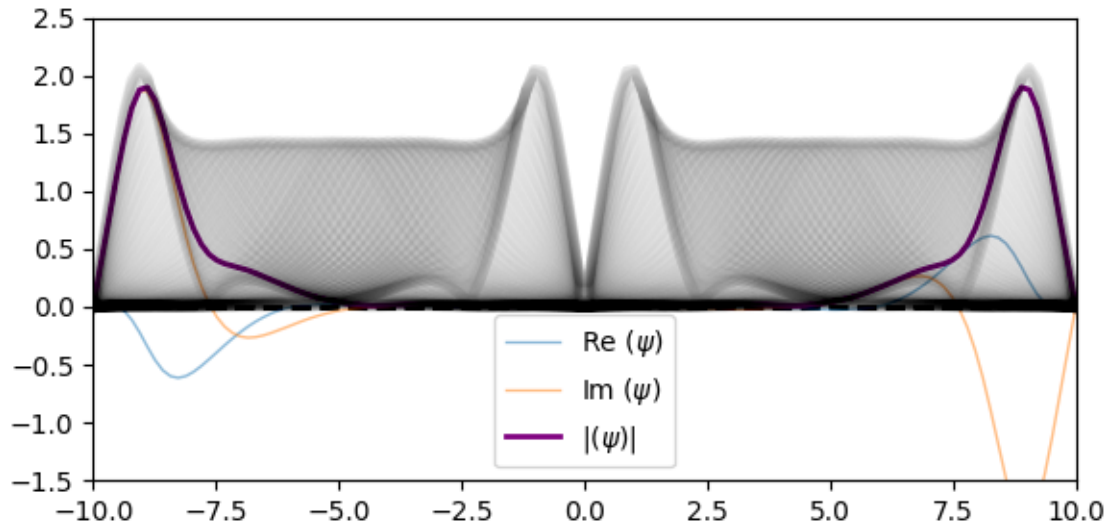
$\frac{\theta}{\pi}$	Minimum Separation	Maximum Separation
0	0	14.02
0.1	2.99	14.02
0.25	4.09	14.02
0.5	5.35	14.02
1	5.83	14.02
1.5	5.35	14.02
1.75	4.09	14.02
1.9	2.99	14.02
2	0	14.02



As we move between these states, we see a gradual transition from symmetry, which has a clear peak at the collision, to the fully separate wave packets of antisymmetry. This effect is periodic, with phases $\theta \in [\pi, 2\pi]$ giving identical behaviour, but mirrored about $x = 0$.

Note also that the phase shift has no effect on the maximum separation. In all cases, each ‘particle’ has the same kinetic energy, and the attraction between these particles means that they are physically bound to each other.

We can more clearly see the way that antisymmetry works like a ‘wall’ by increasing the kinetic energy of the particles:



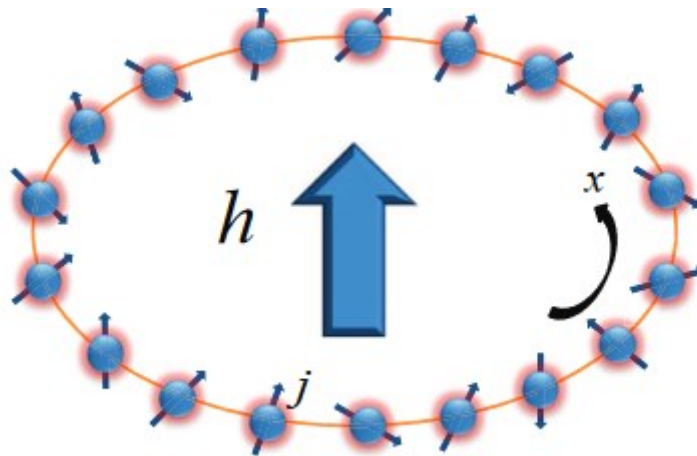
Time evolution of the two wave-packet system for $\theta = \pi$ and $u = 1.0$, showing the wave antisymmetry imposes a node at $x = 0$ that physically separates the two wave-packets.

Part 2 - The Transverse Ising Spin Model

An interesting feature of many-particle systems is their ability to undergo ‘phase changes’, a sudden and discontinuous change in the system behaviour. For such a phase change to be possible, the system’s ground energy, or one of its derivatives, must have a discontinuity.

We can simplify such system as ‘Ising Models’, a discrete grid of particles prepared with different spin-alignments. A simple treatment of these models treats each spin site as a classical particle, being either ‘spin up’ or ‘spin down’. In these classical models, phase changes are observed at for 2 dimensional grids or higher, but not for simple 1D chains of particles.

This simple behaviour is broken when we more properly model our spin sites as quantum particles, allowing them to be in super-positions of spin up and spin down, and in particular when we include the effects of transverse axis spin that arises from superposition. In this section, we consider the 1-dimensional transverse Ising model, in which a closed ring of particles are subject to an external magnetic field in the z-direction, with additional effects arising from the particle-particle interaction via their in-plane spin.



Physical Layout of the Transverse Ising Model – Spin particles in a closed chain with an externally applied potential running ‘across’ the ring. (Deng, Gu, & Chen, 2018)

In a simple system with a single spin-particle, the system energy is related only to how this particle aligns with the external magnetic field. For a field in the positive z-direction, this gives:

$$H = -\sigma_z, \quad \sigma_z = \frac{1}{2} \begin{bmatrix} 1 & 0 \\ 0 & -1 \end{bmatrix}$$

For a system of many spin-particles, we extend this this a simple direct product of their spin operators:

$$H = - \sum_{m=0}^{N-1} \sigma_z^m, \quad \sigma_z^m = I \otimes \dots \frac{1}{2} \begin{bmatrix} 1 & 0 \\ 0 & -1 \end{bmatrix} \dots \otimes I$$

This is a trivial system in which energy is minimized by all particles being spin-up, i.e. aligned with the external field, for an energy of:

$$E_0 = -\frac{1}{2}N$$

However, each particle's z-spin and x-spin are not independent properties. We can also quantify the x-spins of the system:

$$\sigma_x^m = I \otimes \dots \frac{1}{2} \begin{bmatrix} 0 & 1 \\ 1 & 0 \end{bmatrix} \dots \otimes I$$

With additional energy effects based on how these spins align with each other. As a simplified model, we treat this effect as being linear with the interaction between each particle and its nearest neighbour, for a non-linear Hamiltonian:

$$H = - \sum_{m=0}^{N-1} \sigma_z^m - g \sum_{m=0}^{N-1} \sigma_x^m \sigma_x^{m+1}$$

Where, to enforce the periodic 'ring' boundary condition, we set:

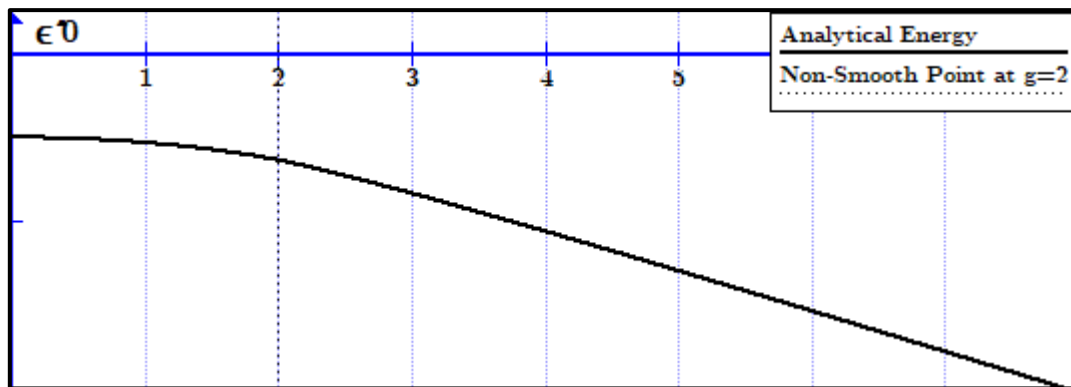
$$\sigma_x^{m=N} = \sigma_x^{m=0}$$

In this pseudo-continuous limit $N \rightarrow \infty$, this Hamiltonian has a well-defined energy for different interaction strengths:

$$\frac{1}{N} \hat{\epsilon}_0(g) = \lim_{N \rightarrow \infty} \frac{1}{N} \epsilon_0 = -\frac{(2+g)}{2\pi} \cdot E\left(\frac{8g}{(2+g)^2}\right), \quad E(x) = \int_0^{\frac{\pi}{2}} \sqrt{1-x \cdot \sin^2(\theta)} \, d\theta$$

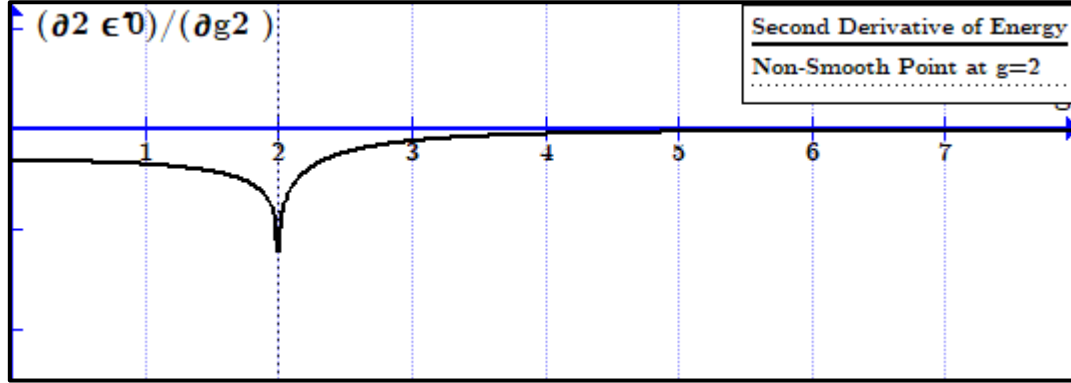
This collapses to the non-interacting case at $g = 0$, while the limit $g \rightarrow \infty$, where particle-particle interaction dominates the energy, the system converges to the case of particles being 'half' aligned with their neighbours on average:

$$\hat{\epsilon}_0(g=0) = -\frac{1}{2}N, \quad \hat{\epsilon}_0(g \rightarrow \infty) = -\frac{1}{4}Ng$$



Graph of Large-N Energy, $\frac{1}{N} \hat{\epsilon}_0(g)$

An important feature of this energy function is that, while the energy itself is smooth and continuous, its higher order derivatives are not. Specifically, the second derivative becomes non-analytic at $g = 2$. Such non analyticity is a sufficient condition for the system to exhibit phase change behaviour.



Graph of $\frac{1}{N} \frac{\partial^2}{\partial g^2} \hat{\epsilon}_0$, the second derivative of large= N energy. At $g = 2$, the function becomes non-analytic, corresponding to a phase change

In this section, we numerically simulate the 1D transverse Ising model, investigating the behaviour of the energy function and its discontinuities for finite-sized systems and the time-evolution of the system and its spin-like properties.

2.1 – Numerical Modelling & Costs of the Transverse Ising Spin Model

To simulate a finite 1D Ising grid, we evaluate the Hamiltonian using:

$$H = H_{dir} + g \cdot H_{int}$$

Where H_{dir} and H_{int} are the direct and interaction Hamiltonian terms:

$$\begin{aligned} H_{dir} &= \frac{1}{2} \sum_{m=0}^{N-1} I(2^m) \otimes \begin{bmatrix} 1 & 0 \\ 0 & -1 \end{bmatrix} \otimes I(2^{N-m-1}) \\ H_{int} &= \frac{1}{2} \sum_{m=0}^{N-2} \left[I(2^m) \otimes \begin{bmatrix} 0 & 1 \\ 1 & 0 \end{bmatrix} \otimes I(2^{N-m-1}) \left[I(2^{m+1}) \otimes \begin{bmatrix} 0 & 1 \\ 1 & 0 \end{bmatrix} \otimes I(2^{N-m-2}) \right] \right] \\ &\quad + \frac{1}{2} \left[\begin{bmatrix} 0 & 1 \\ 1 & 0 \end{bmatrix} \otimes I(2^{N-1}) \left[I(2^{N-1}) \otimes \begin{bmatrix} 0 & 1 \\ 1 & 0 \end{bmatrix} \right] \right] \end{aligned}$$

Where $I(x)$ is an identity matrix of rank ' x '. Note that this leads, for ' N ' atoms, to a matrix of rank 2^N . The last term in H_{int} represents the periodic boundary conditions.

Note that there are two ways to construct the spin-spin interaction terms in the summation. In a simple approach, we calculate each σ_x^m individually, matrix multiply the relevant pairs, and then summate. Alternately, we can avoid the numerically costly matrix multiplication by leveraging some identities with the Kronecker product, i.e.:

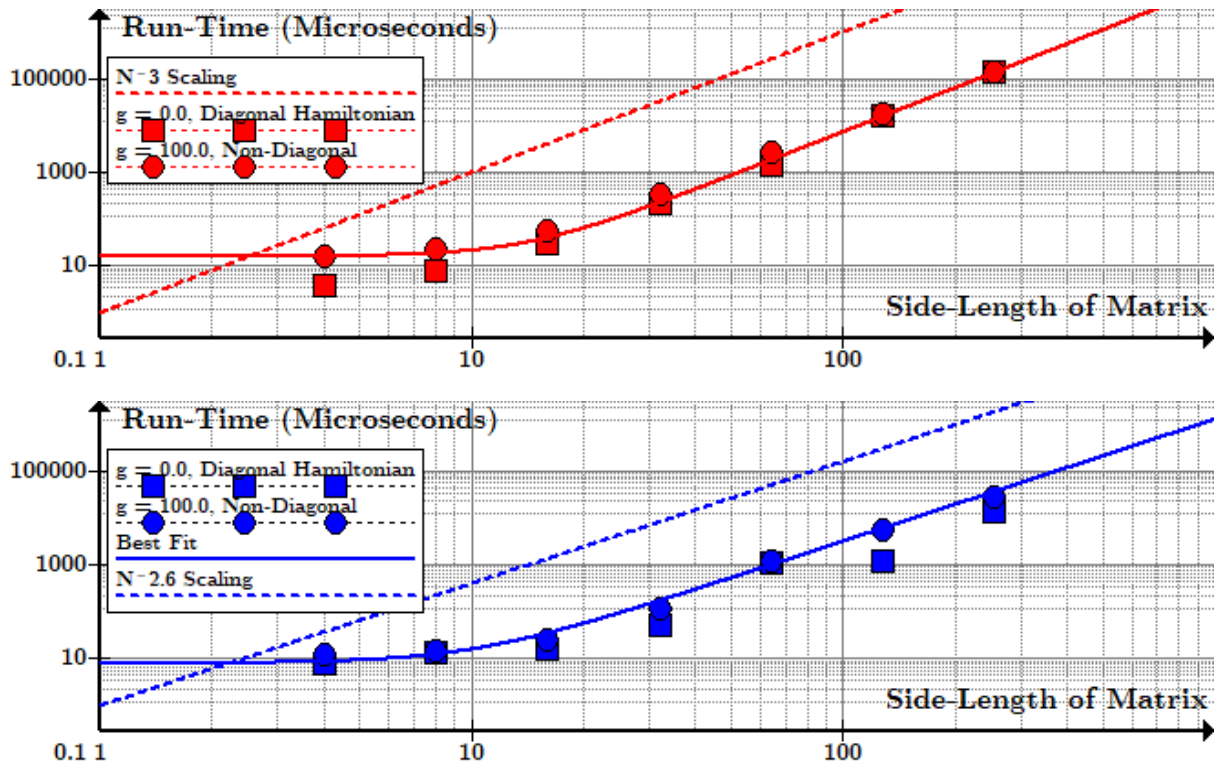
$$\begin{aligned} \sigma_x^m \sigma_x^{m+1} &= I(2^m) \otimes \frac{1}{2} \begin{bmatrix} 0 & 1 \\ 1 & 0 \end{bmatrix} \otimes \frac{1}{2} \begin{bmatrix} 0 & 1 \\ 1 & 0 \end{bmatrix} \otimes I(2^{N-m-2}) \\ &= I(2^m) \otimes \frac{1}{4} \begin{bmatrix} 0 & 0 & 0 & 1 \\ 0 & 0 & 1 & 0 \\ 0 & 1 & 0 & 0 \\ 1 & 0 & 0 & 0 \end{bmatrix} \otimes I(2^{N-m-2}) \end{aligned}$$

The Hamiltonian is constructed using Kronecker products as in the previous section, though there is technically closed forms for finite N . Because the resultant Hamiltonian matrices are sparse, calculation of the eigenstates is relatively low cost compared to similar problems. This means that the cost associated with constructing the Hamiltonian is of large enough impact to be significant.

With the Hamiltonian matrix constructed, the system states and energies are the eigenvectors and eigenvalues of this matrix. We evaluate these with FORTRAN linear algebra routines in LAPACK. The ground energy is then the smallest (most negative) of these values, and the ground state is the corresponding eigenstate.

We test the run-time / complexity scaling against the total matrix size 2^N rather than the number of atoms, as it is this value that is more closely tied to computational cost. Run-times are inclusive of the construction of the Hamiltonian and the ground state evaluation / system diagonalization, and are presented for both a purely diagonal Hamiltonian at $g = 0$ and a strongly interacting system at $g = 100$.

Tracking the runtime for systems with $N = 2, 3, 4, 5, 6, 7$ and 8 atoms, we recover the following:



Computational Runtime (Microseconds, log scale) against matrix size for $g = 0$ and $g = 8$ using Hamiltonian interaction term construction with matrix multiplication (top) and without (bottom)

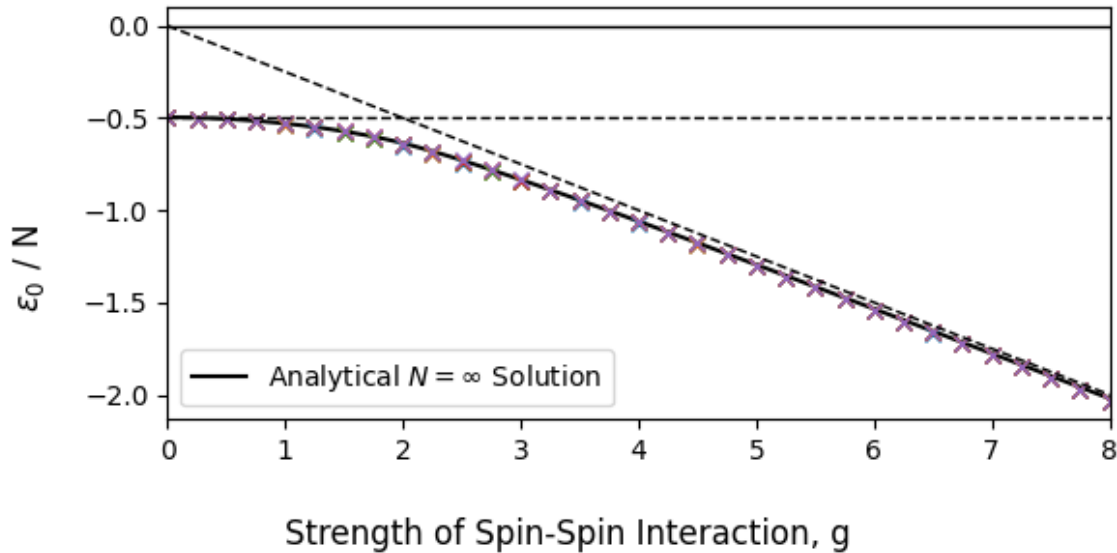
In many similar problems, computational cost is dominated by the diagonalization of the Hamiltonian, but in this case we can see that the large N scaling differs depending on what method we use to construct the interaction term. Diagonal matrices ($g = 0$) yield lower cost, which is to be expected, but as N becomes large this effect becomes small.

We can clearly see that using the matrix-multiplication method for evaluating H_{int} has consistently worse scaling, increasing in cost with $\mathcal{O}(L^3)$, where ' $L = 2^N$ ' is the matrix side length, while the alternate method scales with $\mathcal{O}(L^{2.6})$. By contrast, matrix diagonalization (normally the dominant cost in such problems) has a worst-case scaling of $\mathcal{O}(L^3)$.

2.2 – Effect of Interaction & System Size on Ground Energy Function

Using our simulation, we calculate the ground state energies for systems with atom numbers $N \in [4, 5, 6, 8, 10]$, evaluated at increasing interaction strengths in the domain $g \in [0, 8]$.

Plotting energy against interaction strength for these system scales, we see that they are in near perfect agreement with the analytical $N \rightarrow \infty$ approximation, with all scales following both the $\frac{\epsilon_0}{N} = -\frac{1}{2}$ “all spin up” state at $g = 0$ and converging to the $\frac{\epsilon_0}{N} = -\frac{1}{4}g$ “half up half down” condition at $g \rightarrow \infty$:



Energy per Spin-Site against interaction strength for multiple system scales.
There is almost full overlap between all data series.

What is less consistent with scale is this function’s higher order derivatives. We approximate the derivatives from simulated with the central finite difference equation:

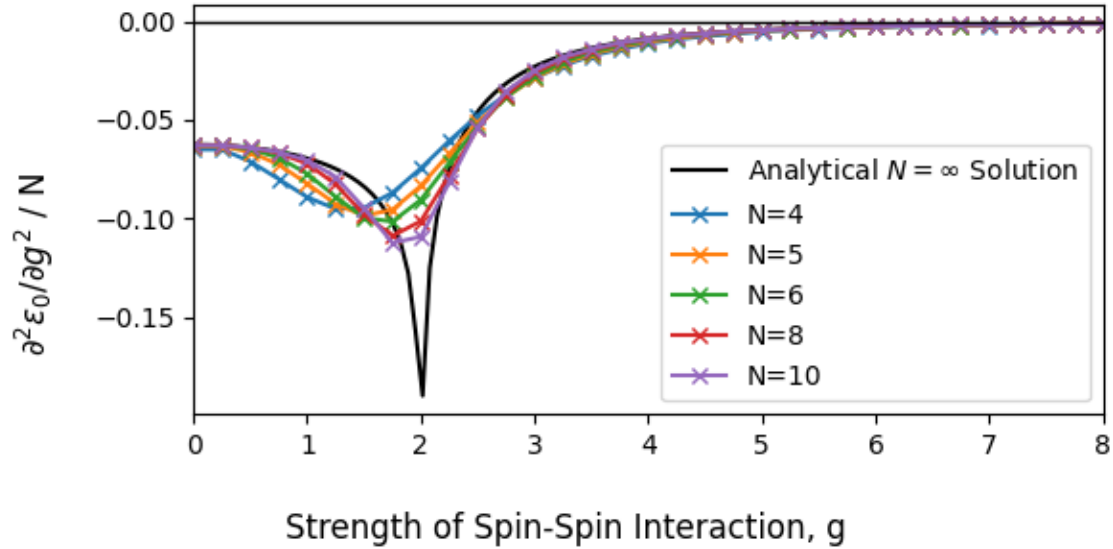
$$\frac{\partial^2 \epsilon_0}{\partial g^2}(g) \approx \frac{\epsilon_0(g + \Delta g) - 2\epsilon_0(g) + \epsilon_0(g - \Delta g)}{\Delta g^2}$$

Note that the first and last terms require us to switch to the forward / backward finite difference approximation, which is equivalent to:

$$\frac{\partial^2 \epsilon_0}{\partial g^2}(g = 0) \approx \frac{\partial^2 \epsilon_0}{\partial g^2}(g = \Delta g), \quad \frac{\partial^2 \epsilon_0}{\partial g^2}(g = g_{Max}) \approx \frac{\partial^2 \epsilon_0}{\partial g^2}(g_{Max} - \Delta g)$$

Where Δg is the interval between our measurements.

Doing so for multiple atom counts, we can see that the phase change behaviour has a much stronger dependence on system scale. The smaller the number of atoms, the “smoother” the curve and less prominent the spike the corresponds to a phase change. In this, the transverse 1D Ising model is similar to the 2D classical Ising model: the less particles to interact, the more gradual the phase change.



Curvature of the energy per spin-site function against interaction strength for multiple system scales

2.3 – Time Evolution of Quenched States

Another area of interest is the response of the Ising model to a change in external conditions. In this section, we examine the effect of changing the interaction strength on the time-evolution of the system. At $g = 0$ (i.e. zero spin-spin interaction) the system’s minimum energy eigenstate is $\psi = (1,0,0, \dots)$, corresponding to all particles being aligned with external magnetic field.

We can model an instantaneous change in the interaction strength by taking this $g = 0$ ground state as an initial condition and seeing how it evolves under a non-zero interaction strength, e.g. $g = 4$. Physically, this ‘turning up’ of the interaction would be more something like ‘turning down’ the direct term, i.e. reducing the external magnetic field so that spin-spin interaction becomes a significant component of the energy.

Though our system is self-interacting, the system is still linear and so we are free to use the linear time evolution operator:

$$|\psi(t)\rangle = K(t) |\psi(t=0)\rangle, \quad K(t) = U e^{-it \cdot D} U^\dagger$$

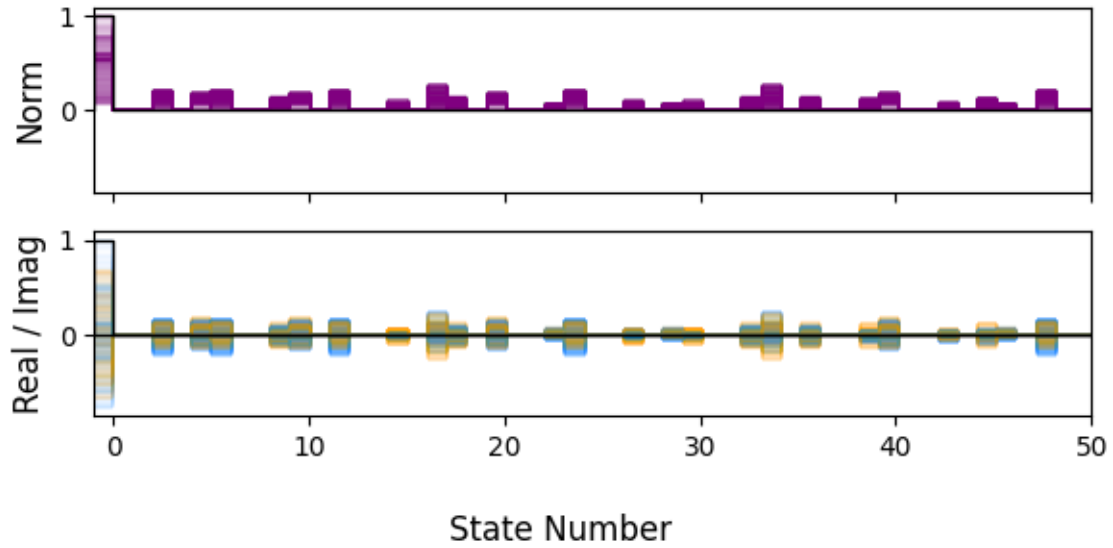
Where U is the matrix constructed from the system eigenvectors $\{|\psi_i\rangle\}$:

$$U = (|\psi_0\rangle, |\psi_1\rangle, \dots)$$

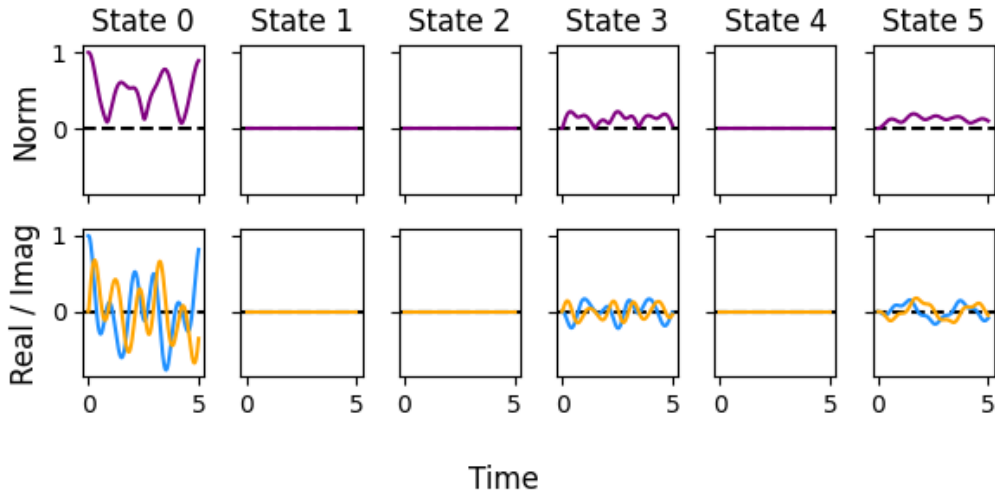
And $e^{-it \cdot D}$ is the exponential matrix:

$$[e^{-itD}]_{ii} = e^{-itE_i}$$

With E_i being the eigenvalue / energy of state i . The $g = 0$ ground state is not an eigenstate of the $g = 4$ system, and so we see the initial $\psi = (1, 0, 0, \dots)$ state ‘bleed’ into external states due to mode mixing. The symmetry of the system and its initial conditions means that only certain modes can be excited, as all particles have the same behaviour (see appendix B).



Overlay of system states evolving in time post-quench. Initial state ($g = 0$ ground state) is marked in black.



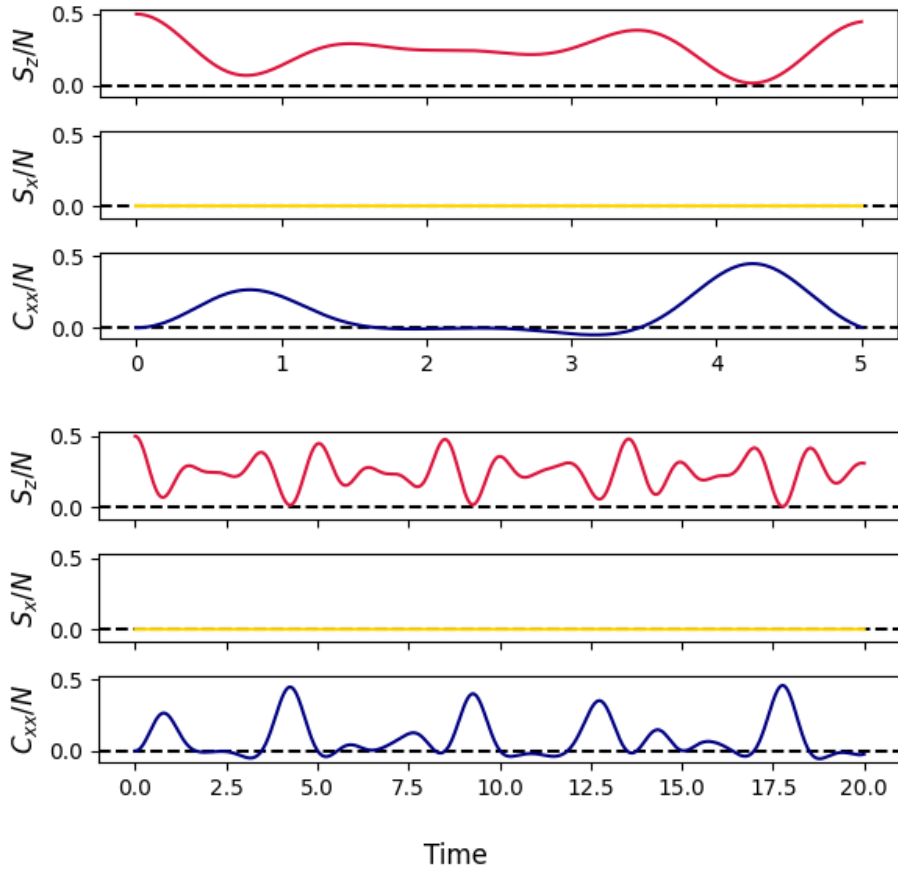
Time-evolution of the first 5 states post-quench

It is also interesting to track the ‘net spin’ and strength of interaction across the system over time. We define the ‘total z-spin’ S_z , ‘total x-spin’ S_x and ‘x-spin interaction’ C_{xx} as:

$$S_z(t) = \langle \psi(t) | \sum_{m=0}^{N-1} \sigma_z^m | \psi(t) \rangle, \quad S_x(t) = \langle \psi(t) | \sum_{m=0}^{N-1} \sigma_x^m | \psi(t) \rangle,$$

$$C_{xx}(t) = \langle \psi(t) | \left[\sum_{n=0, n \neq m}^{N-1} \sum_{m=0}^{N-1} \sigma_x^m \sigma_x^n \right] | \psi(t) \rangle$$

S_z and S_x are easy to interpret: they are just the spin operators for each atom summated, while C_{xx} represents the degree to which the x-spins are aligned between all atom pairs. Calculating these across the systems evolution, we get a fluctuation in S_z , S_x constant at zero, and C_{xx} contra varying with the Z-spin.



Time-Evolution of the Net Spin Observables to $t = 5$ (top) and $t = 20$ (bottom)

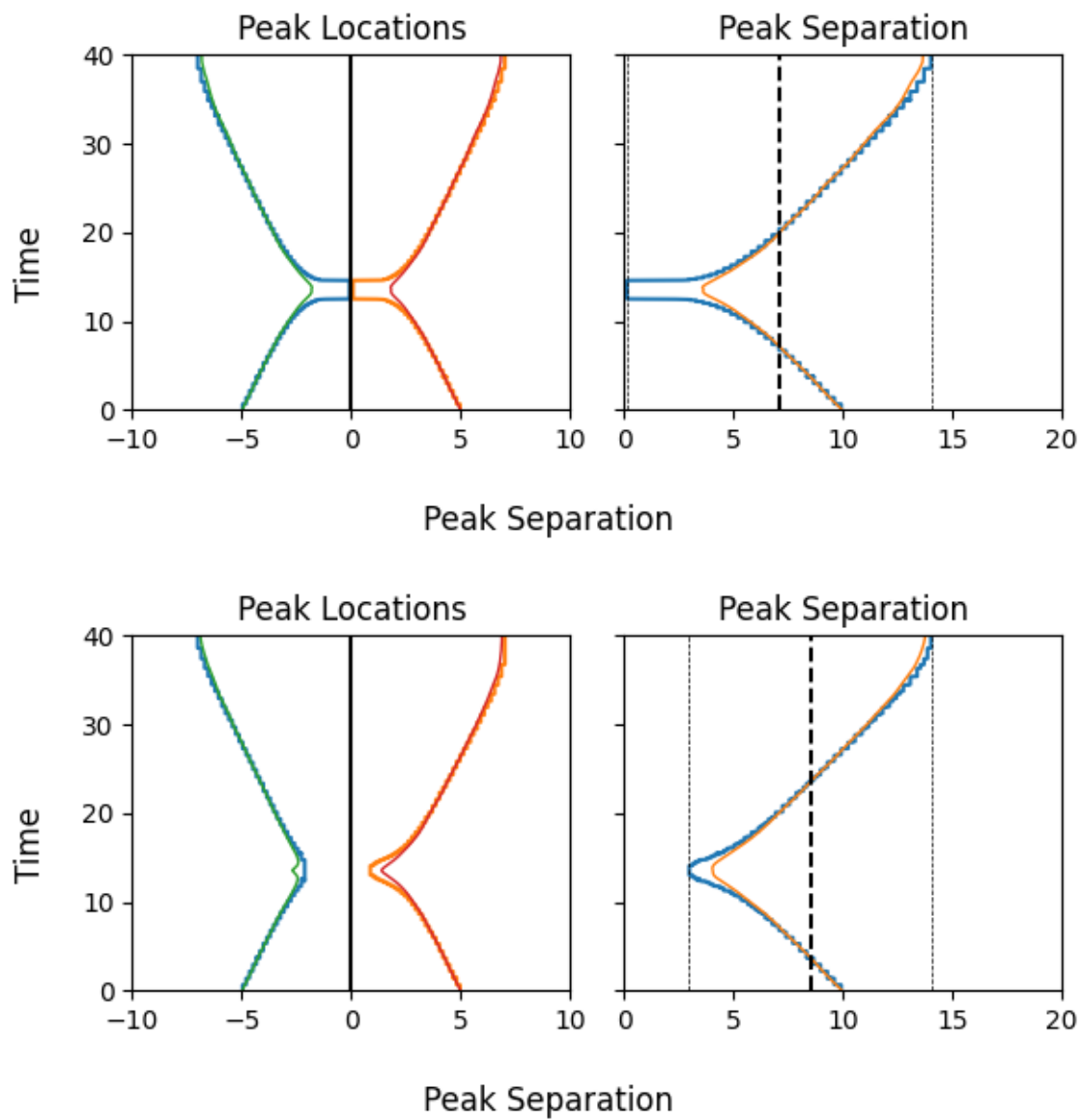
At $t = 0$, the system is prepared in the ‘all spin up’ state, as the pre-quench $g = 0$ state motivates the system to align with the external magnetic field. As such, the z-spin is at its maximum value, while the x-spin related values are all zero. As the system time-evolves it ‘rotates’ into the z-down state, causing S_z to decrease. The symmetry of the system means that the x-up and x-down states are equally excited, meaning S_x remains zero through time. However, C_{xx} becomes non-zero during this transition due as x-spins can still interact through superposition.

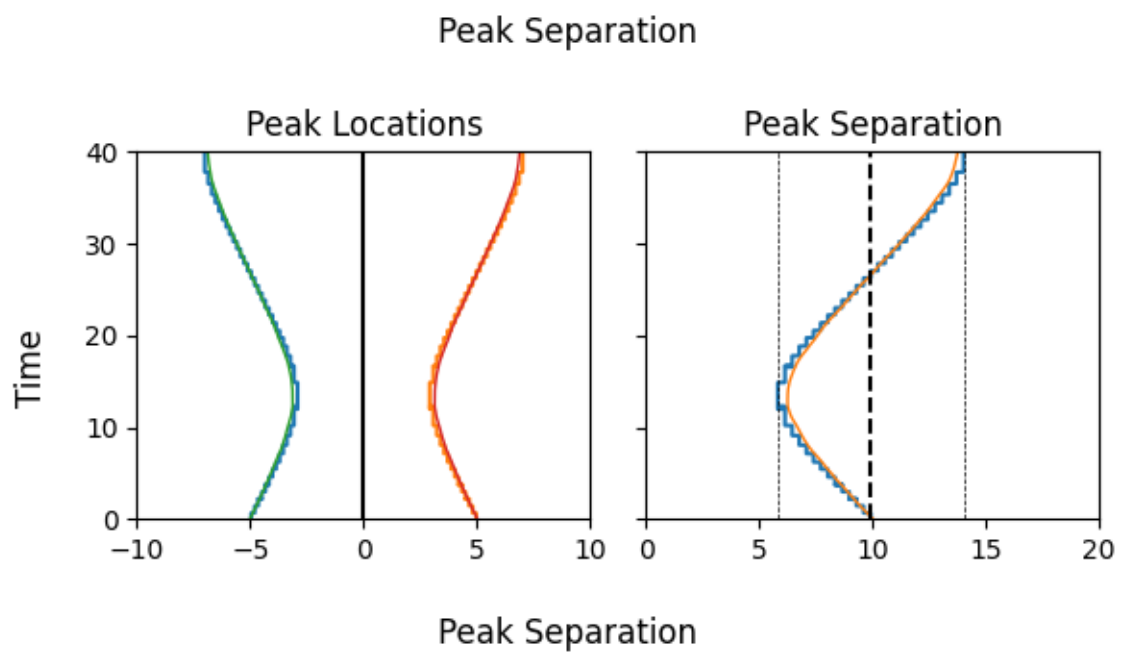
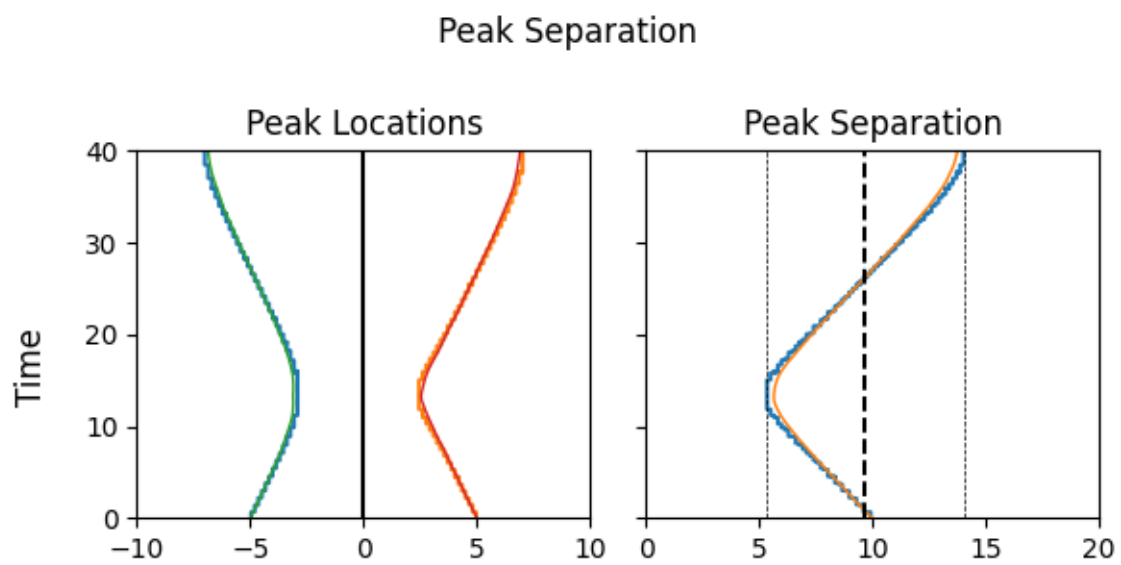
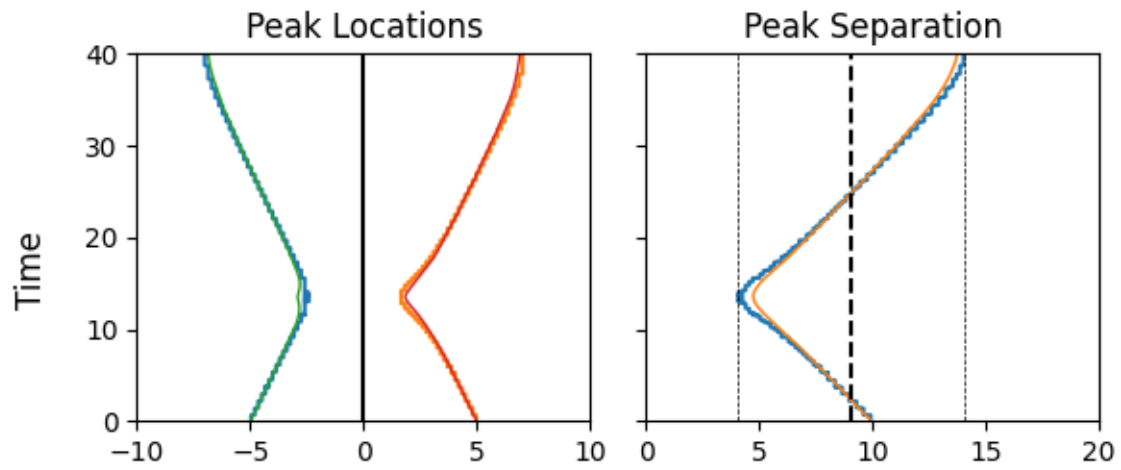
References

Deng, D.-L., Gu, S.-J., & Chen, J.-L. (2018). *Detect genuine multipartite entanglement in the one-dimensional transverse-field*. Chern Institute of Mathematics, Theoretical Physics Division. Tianjin: Nankai University. doi:10.1016/j.aop.2009.09.009

Appendix A – Peak-Peak Separations for All Phase Shifts

Plots of particle peak / mean positions and the inter-particle separations for part 1.4. In order, plots are for $\theta = 0, 0.1\pi, 0.25\pi, 0.5\pi$ and π .





Appendix B – Single Atom Interpretation of the 1D Ising Model

The complex interaction between spin-cites means that a full model of the 1D spin-cite chain has 2^N degrees of freedom, but there is still some interesting in physically interpreting what each individual ‘atom’ is doing. To do so, we need to ‘collapse’ the system to the $2N$ degrees of freedom of each atom’s spin states, losing some important information but gaining some physical intuition in the process. First, note that the full-system elements each describe a string of ‘spin up / spin down’ alignments:

$$\begin{aligned} |\psi\rangle_0 &= (1,0,0,\dots) \rightarrow [\uparrow, \uparrow, \uparrow, \dots] \\ |\psi\rangle_1 &= (0,1,0,\dots) \rightarrow [\downarrow, \uparrow, \uparrow, \dots] \\ |\psi\rangle_2 &= (0,0,1,\dots) \rightarrow [\uparrow, \downarrow, \uparrow, \dots] \end{aligned}$$

As such, the index of each element of $|\psi\rangle$, expressed as a binary number, tells us which spin-up elements it corresponds to, e.g.:

$$|\psi\rangle_5 \rightarrow 0101$$

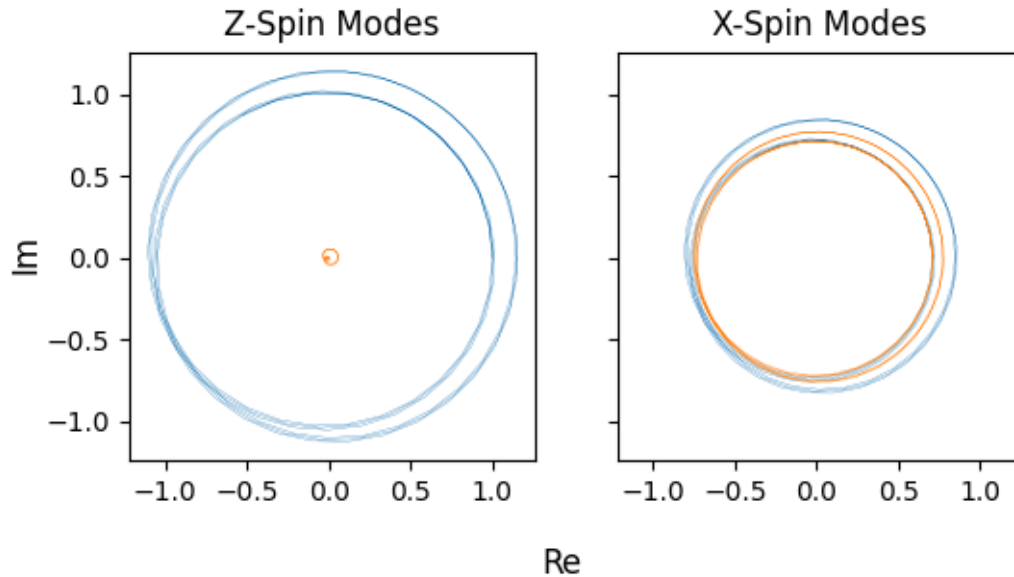
Means that element 5 corresponds to atoms 1 and 3 spin down, atoms 2 and 4 spin up. Using this, we can construct row matrices that add together the contributions of each element of $|\psi\rangle$ to each spin site’s state:

$$A = 1 - B, \quad B = \left[\begin{pmatrix} 0 \\ 0 \\ \vdots \end{pmatrix}, \begin{pmatrix} 1 \\ 0 \\ \vdots \end{pmatrix}, \begin{pmatrix} 0 \\ 1 \\ \vdots \end{pmatrix}, \dots, \begin{pmatrix} 1 \\ 1 \\ \vdots \end{pmatrix} \right]$$

Such that $A|\psi\rangle$ describes the spin-up states of each atom and $B|\psi\rangle$ the spin-down.

Doing so for the quenched state in section 2.3, we find that the collapsed state is the same for all atoms at all times. This is what we expect: we begin with all spin sites “spin up” at $g = 0$ and there is no physically differences to distinguish the cites due to the boundary conditions, and so they should all behave the same.

After collapsing, we can also track the spin-state of each atom. The following is for a weakly interacting system with $g = 0.1$, initialized in the z-spin up state. Plotting for one atom, we can see how the spin states mix with time, as the atom rotates in phase, but shows mixing between the z-up and z-down spin states due to interaction.



This simplified atom-by-atom view does not capture the behaviour of the entire system due a loss of information about phases. For example, while the overall system's x-spin remains zero, the one-atom spin varies slightly out of phase with the z-spin:

